Growth of Walled Cells: From Shells to Vesicles

Arezki Boudaoud*

Department of Mathematics, MIT, 2-335, Cambridge, Massachusetts 02139, USA
and Laboratoire de Physique Statistique de l'ENS, 24, rue Lhomond, 75231 Paris, France
(Received 13 July 2002; published 3 July 2003)

The growth of isolated walled cells is investigated. Examples of such cells range from bacteria to giant algae, and include cochlear hair, plant root hair, fungi, and yeast cells. They are modeled as elastic shells containing a liquid. Cell growth is driven by fluid pressure and is is similar to a plastic deformation of the wall. The requirement of mechanical equilibrium leads to two new scaling laws for cell size that are in quantitative agreement with the compiled biological data. Given these results, possible shapes for growing cells are computed by analogy with those of vesicle membranes.

All cells are enclosed by membranes. Many of them are also bound by protective polymeric walls outside these membranes. For instance, plant cells have walls composed principally of cellulose. The walls sustain the cell shapes as they are much thicker and stiffer than the membranes. Other examples range from bacteria to giant algae and include cochlear hair, fungi, and yeast cells. In this Letter, I study the size and shape of such isolated walled cells. Thompson [1] was a pioneer in explaining forms in nature with physical arguments. He proposed that surface tension alone would determine cell shapes, and his ideas were extended to account for morphogenesis in bacteria and fungi, in the so-called surface stress theory [2,3]. A completely different approach for fungi [4] was based on the concept of ballistic deposition of new material on the wall from a "material supply center." The similarity of the growth patterns of the monocellular algae *micrasterias* with dendritic or diffusion-limited growth has stimulated many theoretical studies. The first [5,6] relied on geometrical models which describe the temporal evolution of the cell wall curvature. These geometrical models were then coupled to the diffusion of morphogens [7]. In the latest [8], the cell wall was considered as an elastic shell which deforms plastically under the influence of a diffusing morphogen. Elastic approaches have also been used for bacteria [9], filamentary bacteria [10], and the algae *acetabularia* [11]. Previous studies obtained only qualitative results and were focused on specific cell types. Here I consider the whole class of walled cells. I demonstrate that a simple model leads to estimations of cell sizes that are in quantitative agreement with biological data and I investigate the possible shapes of these cells.

The starting point is a simplified physical description of a cell (Fig. 1). A liquid (the cytoplasm) is contained in a thin elastic shell (the cell wall). The physical parameters involved are the cell radius of curvature R, the wall thickness h, the elastic modulus of the wall material E, and the pressure P exerted on the wall (or the turgor pressure). The turgor pressure and the thickness of the

wall are mainly regulated by the cell physiology. In the case of plant cells, it has been established [12] that growth is similar to plastic deformations: the wall behaves as an elastic material below a critical strain a_y and grows above by yielding to stress. So, the wall is modeled as a perfectly plastic material [13], which yields in extension and not in compression (see Fig. 1). The cell can also regulate the wall plasticity [12], using hormones such as auxin. When a piece of wall is formed, it has a spontaneous radius of curvature R_0 that it would hold in the absence of external forcing. As there are no other macroscopic length scales, one expects $R_0 \sim R$. Finally, the growth is slow: the characteristic time for growth is much larger than the time needed to reach mechanical equilibrium; consequently, the cell is assumed to be in mechanical equilibrium.

I first estimate the cell mechanical energy. A thin shell has two modes of deformation, stretching and bending [14]. The stretching energy is proportional to the strain
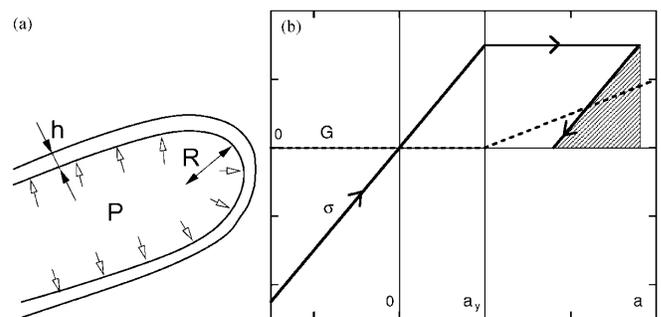
FIG. 1. Physical picture of cell growth. (a) Schematic of a model cell with radius of curvature R and wall thickness h, whose growth is driven by the inner fluid pressure P. (b) Stress-strain $\sigma(a)$ (solid line) and growth rate $G(a)$ (dashed line) curves for the cell wall, which is assumed to be a perfectly plastic material yielding only in extension. The wall is elastic (with modulus E) for a strain a smaller then the yield threshold a_y and it grows above. If the stress is decreased, the released elastic energy (the shaded area) is $1/2 \times Ea_y^2$.

squared, but if the material undergoes plastic deformations (see Fig. 1), then energy is stored only below the yield strain a_y, so the stretching energy (per unit area) scales as

$$E_s \sim Eha_y^2. \tag{1}$$

The elastic energy (per unit area) for bending is proportional to the square of the difference between the mean curvature and the equilibrium curvature $1/R_0 \sim 1/R$,

$$E_b \sim Eh^3(1/R - 1/R_0)^2 \sim Eh^3/R^2. \tag{2}$$

In bending, the outer half of the wall (with respect to the center of curvature) is elongated while the inner half is compressed. When plastic flow occurs, it is restricted to the outer wall, because the material is considered to yield only in extension (Fig. 1). In this case the effective thickness is reduced in the bending energy; however its order of magnitude remains the same. Finally, the potential energy (per unit surface) corresponding to the turgor pressure is proportional to the volume to area ratio,

$$E_t \sim PR. \tag{3}$$

The yield strain for most materials is smaller than 10^{-2}, while the aspect ratio h/R for most cells varies between 10^{-2} and 10^{-1}. So, it is reasonable to consider the limit where $a_y \ll h/R$, so that $E_s \ll E_b$. In this case, a characteristic cell size results from the balance between bending and pressure ($E_b \sim E_t$):

$$R = \alpha h \left(\frac{E}{P}\right)^{1/3}. \tag{4}$$

The best fit to the data compiled in Fig. 2 gives $\alpha = 4.0$. This value is larger than the values $\alpha = 0.58$ and $\alpha = 0.96$ computed in the second part of this paper, but it has the same order of magnitude. This agreement is good given the simplicity of the model; however one might notice a departure from this scaling at small radii (Fig. 2). This motivates the study of the opposite limit $a_y \gg h/R$ for bacteria and cochlear hair cells. Indeed, experiments by Koch (see Ref. [9]) have shown that the typical yield strain for *Bacillus Subtilis* is $a_y = 0.45$. In this limit, stretching balances the turgor pressure. The tension of the shell scales as the yield stress $\gamma \sim Eha_y$ (see Fig. 1). The Laplace law requires $P \sim \gamma/R$, so that

$$R = \beta h \frac{E}{P}. \tag{5}$$

β should be proportional to a_y. The fit to the experimental data (Fig. 3) gives $\beta = 1.0$, of the same order as the values $\beta = 1.8$ and $\beta = 0.9$ estimated below. It has been implicitly assumed that the yield strain a_y varies very little for this class of cells. The forces generated by electric charges have also been neglected, although they could be comparable to the elastic forces [9].

FIG. 2.   Test of the scaling law Eq. (4): cell radius R as a function of $h(E/P)^{1/3}$ (h is the wall thickness, E its elastic modulus, and P the inner pressure). The data were compiled from the literature. When not listed, the lengths were measured from the published photographs. All these cells are cylindrical except the spherical yeast. R is the radius of the cylindrical part of the cell or the radius of the sphere. When E or P was not available, they were replaced by their values for similar species. Alga cells: *Chara corallina* (□) [15,16], *Nitella* (▽) [17–19], and *Acetabularia acetabulum* (◇) [15,16,18–20]. Root hair: *Arabidopis thaliana* (△) [15,18,21,22]. Yeast: *Saccharomyces cerevisiae* (⊞) [23]. Fungi: *Phycomyces* (⊠) [24–26] and *Saprolegnia ferax* (⊙) [24,27,28]. Guinea pig cochlear outer hair cell (●) [29]. Bacteria: *Magnetospirillum gryphiswaldense* (■) [30], *Bacillus subtilis* (◆) [2,9,31], *Escherichia coli* (▲) [32], *Pseudomonas aeruginosa* (▼) [32], and *Saccharopolyspora erythraea* (⊡) [30,33]. Gas vesicles (included for comparison): *Microcystis spirillum* (+) [34] and *Anabeana flosaquae* (×) [34] are small crystalline vesicles found in some bacteria. Solid line: best fit to Eq. (4) of all data except filled symbols and gas vesicles.

As the scaling laws are in agreement with biological data, I now investigate a more quantitative description of cell shapes. The mechanical energy is the sum of the bending, stretching, and pressure energies,

$$E = \frac{1}{2}\kappa \int (c - c_0)^2 dA + \frac{1}{2}E \int \sigma_{ij}a_{ij}dA - PV. \tag{6}$$

The integrals are computed over the cell wall. c is the wall mean curvature, c_0 its spontaneous curvature, σ_{ij} the stress tensor, a_{ij} the strain tensor, and V the cell volume. The bending modulus is [14]

$$\kappa = \frac{Eh^3}{12(1 - \nu^2)}, \tag{7}$$

with ν being the Poisson ratio of the wall material. Most biological materials are nearly incompressible, so that $\nu = 0.5$ will be used for numerical estimates in the following. The stress and strain tensor are related by [14]

$$\sigma_{ij} = \frac{Eh}{1 - \nu^2}[(1 - \nu)a_{ij} + \nu a_{kk}\delta_{ij}]. \tag{8}$$

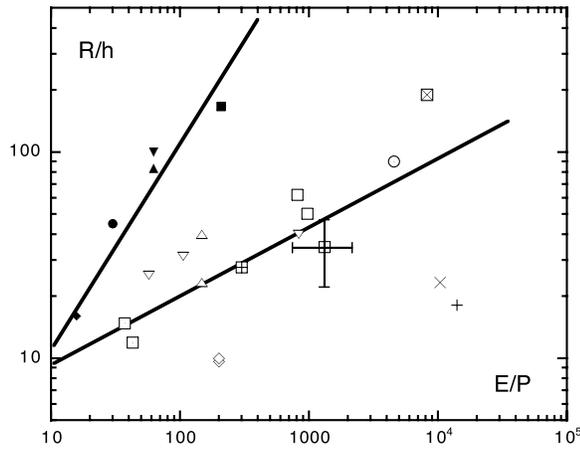Here δ_{ij} is the identity tensor.

FIG. 3. Experimental testing of the scaling laws Eqs. (4) and (5) for cell radii. Cell aspect ratio R/h as a function of the modulus to pressure ratio E/P. Same symbols as in Fig. 2. Solid lines: best fit of filled symbols to Eq. (5) and of all other symbols except gas vesicles to Eq. (4).

I first consider the case where bending balances turgor pressure. Then, the stretching is neglected and the energy has the same form as the energy of a bilayer liquid membrane [35], without the surface tension term. While a complete model should account for variations in c_0 [36], I assume for the sake of simplicity that that c_0 is constant along the wall. The simplest shape for the wall is a sphere of radius R. The equilibrium condition reads [37]

$$PR^3/\kappa = c_0R(c_0R - 2), \qquad (9)$$

so that $c_0 > 2/R$. One would expect c_0 to relax towards the actual curvature $2/R$ [8] and c_0 to assume the smallest possible value. Solving Eq. (9) for c_0 yields $c_0 = f(R)$ whose minimum is reached at a radius R such that $PR^3/\kappa = 8$. So, the largest radius R_0 which a spherical cell would reach corresponds to a prefactor $\alpha = 0.96$ (using $\nu = 0.5$) in the first scaling [Eq. (4)].

If the spontaneous curvature c_0 is large enough, it is known [38] that spherical vesicles are first unstable to prolate ellipsoid shapes. Recall that the wall growth rate increases with the stress which is proportional to the curvature (see Fig. 1). If the cell adopts the shape of a prolate ellipsoid, then the growth rate is larger at the tips (they have the largest curvature). So the cell will become more and more elongated. This is consistent with the observation that most cells which satisfy the scaling of Eq. (4) grow in tubular forms (capped cylinders).

As a limiting case, I now examine the possibility of tubular growth within the present framework. One can seek axisymmetric shapes intersecting the symmetry axis z and matching (possibly for $z \to \infty$) a cylinder of unknown radius R. Let ψ be the angle of the surface normal to the z axis and r the radial coordinate. If the curvature $d(\sin\psi)/dr + \sin\psi/r$ is bounded then Ref. [37] gives

$$\psi'' = \frac{1}{2}\tan\psi(\psi')^2 - \frac{1}{r}\psi' + \frac{1}{r^2}\tan\psi - \frac{PR^3}{\kappa}\frac{r}{2\cos^3\psi}$$

$$+ \frac{\sin\psi}{2\cos^3\psi}\left(\frac{\sin\psi}{r} - c_0R\right)^2. \qquad (10)$$

The primes stand for derivatives with respect to r and lengths are nondimensionalized by the radius R. The first boundary condition at the axis is $\psi(0) = 0$. Following biological observations [4,39], most of the growth occurs at the tip. As a consequence the unknown spontaneous curvature c_0 should be equal to the curvature at the tip: $\psi'(0) = c_0R/2$. At the cylinder, $\psi(1) = \pi/2$, and the curvature is 1 (in R units): $d(\sin\psi)/dr(r = 1) = 0$. There are two extra boundary conditions because both c_0R and PR^3/κ are unknown. A numerical shooting leads to the solution represented in Fig. 4 where $z(r)$ is obtained by integration:

$$\frac{dz}{dr} = -\tan\psi. \qquad (11)$$

The values $c_0 = 2.34/R$ and $PR^3/\kappa = 1.79$ are found. This is consistent with the scaling $c_0 \sim 1/R$ used in the analysis. Using a reasonable Poisson ratio $\nu = 0.5$, one gets as a prefactor of Eq. (4) $\alpha = 0.58$. Moreover, the resulting cylindrical shapes are stable as $c_0R \gtrsim 1$ (see [38]).

In the second case, stretching balances pressure and the first term in Eq. (6) is negligible. If growth occurs all over the wall, the yield strain is reached: $a_{ij} = a_y\delta_{ij}$. Equation (8) gives an isotropic stress $\sigma_{ij} = \gamma\delta_{ij}$, and
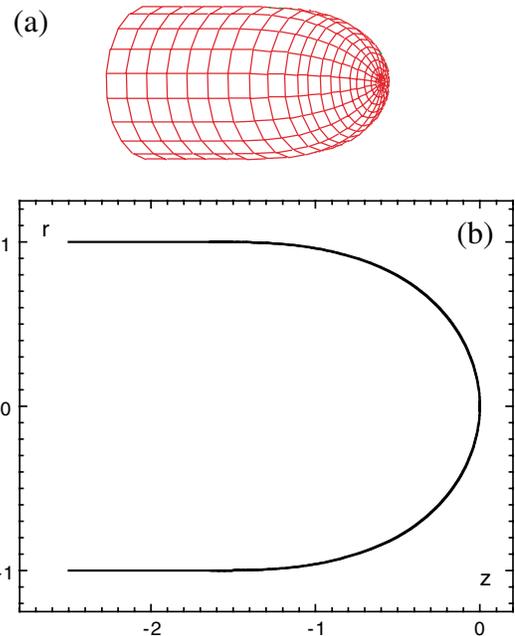

FIG. 4 (color online). Shape $z(r)$ of a tip growing cell according to Eqs. (10) and (11). The surface is axisymmetric with respect to the z axis and matches onto a cylinder. Lengths are nondimensionalized by the radius of the cylinder. (a) 3D view. (b) Cut along a plane of symmetry.

there is an effective surface tension

$$\gamma = \frac{Eha_y}{1 - \nu}.$$ (12)

The problem is equivalent to soap bubbles with internal pressure; therefore the only possible shapes are spheres such that $P = 2\gamma/R$, so that the prefactor of the second scaling [Eq. (5)] is $\beta = 1.8$ (using $\nu = 0.5$). It is likely that anisotropies are necessary to explain the cylindrical shapes of many bacteria [36]. If the shape is cylindrical, $P = \gamma/R$, and a smaller estimation of the prefactor is obtained: $\beta = 0.9$.

To summarize, the size of isolated walled cells obey one of two scalings depending on the plastic properties of the wall. In the first case, bending balances turgor pressure and tip growth occurs. In the second case, stretching balances turgor and there is diffuse growth. A number of physical effects have been neglected but will be the subject of future work [36]. In particular, the spontaneous curvature of the wall is generally not constant and its temporal evolution should be considered. Also, anisotropies in growth or in the wall elastic properties are likely to be important for cell shapes especially in the second class of cells. The subject seems promising as this simple model accounts for many biological observations.

---

*Electronic address: boudaoud@lps.ens.fr

[1] D. A. Thompson, *On Growth and Form* (Cambridge University Press, Cambridge, 1942).
[2] A. L. Koch, Adv. Microb. Physiol. **24**, 301 (1983).
[3] A. L. Koch, J. Theor. Biol. **171**, 137 (1994).
[4] G. Gierz and S. Bartnicki-Garcia, J. Theor. Biol. **208**, 151 (2001).
[5] P. Pelcé and A. Pocheau, J. Theor. Biol. **156**, 197 (1992).
[6] P. Pelcé and J. Sun, J. Theor. Biol. **160**, 375 (1993).
[7] B. Denet, Phys. Rev. E **53**, 986 (1996).
[8] R. Kam and H. Levine, Phys. Rev. Lett. **79**, 4290 (1997).
[9] J. J. Thwaites and N. H. Mendelson, Adv. Microb. Physiol. **32**, 123 (1999).
[10] A. Goriely and M. Tabor, Phys. Rev. Lett. **90**, 108101 (2003).
[11] C. R. Steele, J. Appl. Mech. **67**, 237 (2000).
[12] D. Cosgrove, Annu. Rev. Plant Physiol. **37**, 377 (1986).
[13] W. Johnson and P. B. Mellor, *Engineering Plasticity* (Ellis Horwood, Chichester, 1983).
[14] L. D. Landau and E. M. Lifshitz, *Theory of Elasticity* (Pergamon Press, New York, 1986).
[15] G. A. Toole, P. A. Gunning, M. L. Parker, A. C. Smith, and K.W. Waldron, Planta **212**, 606 (1999).
[16] T. E. Proseus, J. K. E. Ortega, and J. S. Boyer, Plant Physiol. **119**, 775 (1999).
[17] M. C. Probine and R. D. Preston, J. Exp. Bot. **13**, 111 (1962).
[18] N. Kamiya, M. Tawawa, and T. Takata, Protoplasma **57**, 501 (1963).
[19] P. B. Green, R. O. Erickson, and J. Buggy, Plant Physiol. **47**, 423 (1971).
[20] J. Dumais and L. G. Harrison, Philos. Trans. R. Soc. London, Ser. B **355**, 281 (2000).
[21] R. R. Lew, Plant Physiol. **112**, 1089 (1996).
[22] M. E. Galway, D. C. Lane, and J.W. Schiefelbein, Can. J. Bot. **77**, 494 (1999).
[23] A. E. Smith, K. E. Moxham, and A. P. J. Middelberg, Chem. Eng. Sci. **55**, 2043 (2000).
[24] C. N. Ahlquist and R. I. Gamow, Plant Physiol. **51**, 586 (1973).
[25] J. K. E. Ortega, E. G. Zehr, and R. G. Keanini, Biophys. J. **56**, 465 (1989).
[26] C. N. Ahlquist, S. C. Iverson, and W. E. Jasman, J. Biomechanics **8**, 357 (1975).
[27] N. P. Money and F. M. Harold, Planta **190**, 426 (1993).
[28] I. B. Heath and S. G.W. Kaminskyh, J. Cell Sci. **93**, 41 (1989).
[29] W. E. Brownell, A. A. Spector, R. M. Raphael, and A. S. Popel, Annu. Rev. Biomed. Eng. **3**, 169 (2001).
[30] M. Arnoldi, M. Fritz, E. Bäuerlein, M. Radmacher, E. Sackmann, and A. Boulbitch, Phys. Rev. E **62**, 1034 (2000).
[31] A. M. Whatmore and R. H. Reed, J. Gen. Microbiol. **136**, 2521 (1990).
[32] X. Yao, M. Jericho, D. Pink, and T. Beveridge, J. Bacteriol. **181**, 6865 (1999).
[33] S. M. Stocks and C. R. Thomas, Biotech. Bioeng. **73**, 370 (2001).
[34] A. E. Walsby, J. Gen. Microbiol. **137**, 2401 (1991).
[35] W. Helfrich, Z. Naturforsch. **28C**, 693 (1973).
[36] A. Boudaoud (to be published).
[37] W.-M. Zheng and J. Liu, Phys. Rev. E **48**, 2856 (1993).
[38] O.-Y. Zhong-can and W. Helfrich, Phys. Rev. A **39**, 5280 (1989).
[39] P. B. Green, Annu. Rev. Plant Physiol. **20**, 365 (1969).